Pergamon

Int. J. Solids Structures Vol. 35, No. 17, pp. 2183–2203, 1998

0020–7683/98 $19.00 + .00

PII: S0020–7683(97)00183-2

SCATTERING OF OBLIQUE FLEXURAL WAVES BY A THROUGH CRACK IN A CONDUCTING MINDLIN PLATE IN A UNIFORM MAGNETIC FIELD

YASUHIDE SHINDO and SHINGO TOHYAMA
Department of Materials Processing, Graduate School of Engineering, Tohoku University, Sendai 980-77, Japan

(*Received* 10 *February* 1997; *in revised form* 14 *June* 1997)

Abstract—This paper deals with the scattering of time harmonic flexural waves by a through crack in a conducting plate under a uniform magnetic field normal to the crack surface. This study is based on Mindlin's theory of plate bending for magneto–elastic interactions under a quasistatic electromagnetic field. It is assumed that the plate has finite and electric conductivity, and the electric and magnetic permeabilities of free space. An incident wave giving rise to moments symmetric about the crack plane is applied in an arbitrary direction. Fourier transforms are used to reduce the mixed boundary value problem to one involving the numerical solution of Fredholm integral equations. The dynamic moment intensity factor vs frequency is computed and the influence of the magnetic field and the angle of incidence on the normalized values is displayed graphically. © 1998 Elsevier Science Ltd.

1. INTRODUCTION

Recently, great interest has been shown in the dynamic crack problems of magneto–elasticity. The study of these problems is motivated by their importance in the field of applied super-conductivity. The dynamic behavior of a cracked electrically conducting elastic plate is sufficiently affected by the presence of the strong magnetic field. Shindo *et al.* have considered the scattering of time harmonic flexural waves by a through crack in a conducting plate under a uniform magnetic field normal to the crack surface for two special cases, perfect conductivity (Shindo *et al.*, 1993) and quasistatic electromagnetic field (Shindo *et al.*, 1995), which are of physical interest.

The present paper presents the scattering of time harmonic flexural waves by a through crack in a conducting Mindlin plate under a uniform magnetic field to show the effect of magnetic damping by induced current on the wave motion. Mindlin's theory of plate bending (Mindlin, 1951) for magneto–elastic interactions in conducting bodies, which accounts for the rotatory inertia and shear effects, is applied. The plate is engulfed by a uniform magnetic field directed normal to the crack and subjected to incident waves that generate vibratory motion in the transverse direction of the plate. Although the solutions of the present paper concern, in principle, the quasistatic electromagnetic field, they can be used to obtain approximate appraisal of the influence of finite electric conductivity. A solution of the magneto–elastic crack problem is obtained by the method of dual integral equations and the result is expressed in terms of a Fredholm integral equation of the second kind that is amenable to numerical calculations. Numerical solutions are obtained for the dynamic moment intensity factor, and are displayed graphically as the parameters of the frequency, the magnetic field and the angle of incidence are varied.

2. MAGNETO–ELASTIC INTERACTIONS AND MINDLIN PLATE BENDING

We consider an electrically conducting elastic plate of thickness $2h$ with finite electric conductivity. The coordinate axes x and y are in the middle plane of the plate and the z-axis is perpendicular to this plane. It is assumed that the plate has the electric and magnetic permeabilities $\varepsilon = \varepsilon_0 = 8.85 \times 10^{-12}$ F/m, $\kappa = \kappa_0 = 1.26 \times 10^{-6}$ H/m, respectively, with ε_0

and κ_0 being the free space permeabilities. The conducting plate is permeated by a static uniform magnetic field $\mathbf{H}_0$. We consider small perturbations characterized by the displacement vector $\mathbf{u}$ produced in the plate. The magnetic field may be expressed in the form

$$\mathbf{H} = \mathbf{H}_0 + \mathbf{h},$$
$$\mathbf{E} = \mathbf{0} + \mathbf{e}, \tag{1}$$

where $\mathbf{H}$ and $\mathbf{E}$ are the magnetic and electric field intensity vectors, and $\mathbf{h}$ and $\mathbf{e}$ are the fluctuating fields and are assumed to be of the same order of magnitude as the particle displacement $\mathbf{u}$.

Neglecting displacement currents compared to the conduction currents, we have the following linearized field equations (Dunkin and Eringen, 1963):

$$\operatorname{curl} \mathbf{e} = -\kappa_0 \mathbf{h}_{,t}, \tag{2}$$

$$\operatorname{curl} \mathbf{h} = \mathbf{j}, \tag{3}$$

$$\operatorname{div} \mathbf{h} = \mathbf{0}, \tag{4}$$

$$\operatorname{div} \mathbf{e} = \mathbf{0}, \tag{5}$$

$$\sigma_{xx,x} + \sigma_{yx,y} + \sigma_{zx,z} + (\mathbf{j} \times \mathbf{B}_0)_x = \rho u_{x,tt},$$
$$\sigma_{xy,x} + \sigma_{yy,y} + \sigma_{zy,z} + (\mathbf{j} \times \mathbf{B}_0)_y = \rho u_{y,tt},$$
$$\sigma_{xz,x} + \sigma_{yz,y} + \sigma_{zz,z} + (\mathbf{j} \times \mathbf{B}_0)_z = \rho u_{z,tt}, \tag{6}$$

where a comma denotes partial differentiation with respect to the coordinate or the time t, $\mathbf{j}$ is the current density, $\mathbf{B}_0 = \kappa_0 \mathbf{H}_0$ is the magnetic induction, ρ is the mass density, $(\sigma_{xx}, \sigma_{yy}, \sigma_{zz}, \sigma_{xy} = \sigma_{yx}, \sigma_{yz} = \sigma_{zy}, \sigma_{zx} = \sigma_{xz})$ are the elastic stress components, and (u_x, u_y, u_z) are the components of $\mathbf{u}$. In a moving conductor the current is determined by Ohm's law as

$$\mathbf{j} = \sigma(\mathbf{e} + \mathbf{u}_{,t} \times \mathbf{B}_0), \tag{7}$$

where σ is the electric conductivity. The mechanical constitutive equations are taken to be the usual Hooke's law

$$\sigma_{xx} = \lambda(u_{x,x} + u_{y,y} + u_{z,z}) + 2\mu u_{x,x},$$
$$\sigma_{yy} = \lambda(u_{x,x} + u_{y,y} + u_{z,z}) + 2\mu u_{y,y},$$
$$\sigma_{zz} = \lambda(u_{x,x} + u_{y,y} + u_{z,z}) + 2\mu u_{z,z},$$
$$\sigma_{xy} = \mu(u_{x,y} + u_{y,x}),$$
$$\sigma_{yz} = \mu(u_{y,z} + u_{z,y}),$$
$$\sigma_{xz} = \mu(u_{z,x} + u_{x,z}), \tag{8}$$

where λ, μ are the Lamé constants. Outside the plate the external fields are solutions of

$$\operatorname{curl} \mathbf{e}^{\mathrm{e}} = -\kappa_0 \mathbf{h}^{\mathrm{e}}_{,t}, \tag{9}$$

$$\operatorname{curl} \mathbf{h}^{\mathrm{e}} = \mathbf{0}, \tag{10}$$

$$\operatorname{div} \mathbf{h}^{\mathrm{e}} = \mathbf{0}, \tag{11}$$

$$\operatorname{div} \mathbf{e}^e = \mathbf{0}, \tag{12}$$

where the superscript e denotes the external value of the quantity so labeled.

From eqns (2)–(7), we have the field equations:

$$e_{z,y} - e_{y,z} = -\kappa_0 h_{x,t}, \tag{13}$$

$$e_{x,z} - e_{z,x} = -\kappa_0 h_{y,t}, \tag{14}$$

$$e_{y,x} - e_{x,y} = -\kappa_0 h_{z,t}, \tag{15}$$

$$h_{z,y} - h_{y,z} = \sigma[e_x + \kappa_0(H_{0z}u_{y,t} - H_{0y}u_{z,t})], \tag{16}$$

$$h_{x,z} - h_{z,x} = \sigma[e_y + \kappa_0(H_{0x}u_{z,t} - H_{0z}u_{x,t})], \tag{17}$$

$$h_{y,x} - h_{x,y} = \sigma[e_z + \kappa_0(H_{0y}u_{x,t} - H_{0x}u_{y,t})], \tag{18}$$

$$h_{x,x} + h_{y,y} + h_{z,z} = 0, \tag{19}$$

$$e_{x,x} + e_{y,y} + e_{z,z} = 0, \tag{20}$$

$$\sigma_{xx,x} + \sigma_{xy,y} + \sigma_{xz,z} = \rho u_{x,tt} + \sigma\{-\kappa_0 H_{0z}e_y + \kappa_0 H_{0y}e_z + \kappa_0^2[(H_{0z}^2 + H_{0y}^2)u_{x,t} - H_{0x}H_{0z}u_{z,t} - H_{0x}H_{0y}u_{y,t}]\}, \tag{21}$$

$$\sigma_{xy,x} + \sigma_{yy,y} + \sigma_{yz,z} = \rho u_{y,tt} + \sigma\{-\kappa_0 H_{0x}e_z + \kappa_0 H_{0z}e_x + \kappa_0^2[(H_{0x}^2 + H_{0z}^2)u_{y,t} - H_{0x}H_{0y}u_{x,t} - H_{0y}H_{0z}u_{z,t}]\}, \tag{22}$$

$$\sigma_{xz,x} + \sigma_{yz,y} + \sigma_{zz,z} = \rho u_{z,tt} + \sigma\{-\kappa_0 H_{0y}e_x + \kappa_0 H_{0x}e_y + \kappa_0^2[(H_{0x}^2 + H_{0y}^2)u_{z,t} - H_{0y}H_{0z}u_{y,t} - H_{0x}H_{0z}u_{x,t}]\}, \tag{23}$$

where (H_{0x}, H_{0y}, H_{0z}), (e_x, e_y, e_z) and (h_x, h_y, h_z) are the components of $\mathbf{H}_0$, $\mathbf{e}$ and $\mathbf{h}$.

If the conducting plate is set into steady-state motion by the propagating flexural waves, the rectangular components of the displacement vector may assume the forms

$$u_x = z\Psi_x(x, y, t), \quad u_y = z\Psi_y(x, y, t), \quad u_z = \Psi_z(x, y, t). \tag{24}$$

The normal displacement of the plate is Ψ_z and rotations of the normals about the x- and y-axes are denoted by Ψ_x and Ψ_y. By using the theory of magnetoelastic plate bending (Ambartsumian *et al.*, 1971, 1975), the x, y-components of $\mathbf{e}$ and the z-component of $\mathbf{h}$ may be expressed as follows:

$$e_x = \varphi(x, y, t), \quad e_y = \psi(x, y, t), \quad h_z = f(x, y, t), \tag{25}$$

in which φ, ψ, f are the functions of x, y, t. Substituting eqns (24) and (25) into eqns (16), (17) and (20) yields

$$h_{x,z} = f_{,x} + \sigma[\psi + \kappa_0(H_{0x}\Psi_{z,t} - zH_{0z}\Psi_{x,t})], \tag{26}$$

$$h_{y,z} = f_{,y} - \sigma[\varphi - \kappa_0(H_{0y}\Psi_{z,t} - zH_{0z}\Psi_{y,t})], \tag{27}$$

$$e_{z,z} = -\varphi_{,x} - \psi_{,y}. \tag{28}$$

The linearized electromagnetic boundary conditions are also obtained as

$$
\begin{aligned}
h_x(x,y,\pm h,t) &= h^e_x(x,y,\pm h,t),\\
h_y(x,y,\pm h,t) &= h^e_y(x,y,\pm h,t),\\
f(x,y,t) &= h^e_z(x,y,\pm h,t),
\end{aligned}
\tag{29}
$$

$$
\begin{aligned}
\varphi(x,y,t) &= e^e_x(x,y,\pm h,t),\\
\psi(x,y,t) &= e^e_y(x,y,\pm h,t),\\
e_z(x,y,\pm h,t) &= e^e_z(x,y,\pm h,t).
\end{aligned}
\tag{30}
$$

Taking into account the boundary conditions (29) and (30) and integrating the representations (26)–(28) with respect to z, we obtain the remaining electromagnetic field components as

$$
\begin{aligned}
h_x &= \frac{h_x(x,y,h,t)+h_x(x,y,-h,t)}{2} + z[f_{,x}+\sigma(\psi+\kappa_0 H_{0x}\Psi_{z,t})]\\
&\quad -\sigma\kappa_0 H_{0z}\frac{z^2-h^2}{2}\Psi_{x,t},\\
h_y &= \frac{h_y(x,y,h,t)+h_y(x,y,-h,t)}{2} + z[f_{,y}-\sigma(\varphi-\kappa_0 H_{0y}\Psi_{z,t})]\\
&\quad -\sigma\kappa_0 H_{0z}\frac{z^2-h^2}{2}\Psi_{y,t},
\end{aligned}
\tag{31}
$$

$$
e_2 = \frac{e_z(x,y,h,t)+e_z(x,y,-h,t)}{2} - z(\varphi_{,x}+\psi_{,y}). \tag{32}
$$

Therefore, all the electromagnetic field components are represented by means of the six desired functions φ, ψ, f, Ψ_x, Ψ_y, Ψ_z. Substituting eqns (24) and (25) into the eqns (26), (27) and (15), and integrating the equations with respect to z from $-h$ to h, we have

$$
f_{,x}+\sigma(\psi+\kappa_0 H_{0x}\Psi_{z,t}) = \frac{h_x(x,y,h,t)-h_x(x,y,-h,t)}{2h}, \tag{33}
$$

$$
f_{,y}-\sigma(\varphi-\kappa_0 H_{0y}\Psi_{z,t}) = \frac{h_y(x,y,h,t)-h_y(x,y,-h,t)}{2h}, \tag{34}
$$

$$
\psi_{,x}-\varphi_{,y} = -\kappa_0 f_{,t}. \tag{35}
$$

The bending and twisting moments per unit length ($M_{xx}, M_{yy}, M_{xy} = M_{yx}$) and the vertical shear forces per unit length (Q_x, Q_y) can be expressed in terms of Ψ_x, Ψ_y and Ψ_z as

$$
\begin{aligned}
M_{xx} &= \int_{-h}^{h} z\sigma_{xx}\,dz = D(\Psi_{x,x}+\nu\Psi_{y,y}),\\
M_{yy} &= \int_{-h}^{h} z\sigma_{yy}\,dz = D(\Psi_{y,y}+\nu\Psi_{x,x}),\\
M_{xy} = M_{yx} &= \int_{-h}^{h} z\sigma_{xy}\,dz = \frac{(1-\nu)}{2}D(\Psi_{y,x}+\Psi_{x,y}),
\end{aligned}
\tag{36}
$$

$$Q_x = \int_{-h}^{h} \sigma_{xz}\,dz = \frac{\pi^2}{6}\mu h(\Psi_{z,x}+\Psi_x),$$

$$Q_y = \int_{-h}^{h} \sigma_{yz}\,dz = \frac{\pi^2}{6}\mu h(\Psi_{z,y}+\Psi_y), \tag{37}$$

where $D = 4\mu h^3/3(1-\nu)$ is the flexural rigidity of the plate and ν is the Poisson's ratio. The stress boundary conditions on the plate surfaces are

$$\sigma_{xz} = \sigma_{yz} = \sigma_{zz} = 0 \quad (z = \pm h). \tag{38}$$

Now if we multiply eqns (21) and (22) by $z\,dz$ and integrate from $-h$ to h, taking into account the boundary condition (38), we shall obtain the results

$$M_{xx,x} + M_{xy,y} - Q_x = \frac{2}{3}\rho h^3 \Psi_{x,tt} - m_{xx}, \tag{39}$$

$$M_{xy,x} + M_{yy,y} - Q_y = \frac{2}{3}\rho h^3 \Psi_{y,tt} - m_{yy}. \tag{40}$$

The moments m_{xx} and m_{yy} are derived as

$$m_{xx} = -\frac{2}{3}\sigma\kappa_0 h^3\{\kappa_0[(H_{0z}^2 + H_{0y}^2)\Psi_{x,t} - H_{0x}H_{0y}\Psi_{y,t}] - H_{0y}(\varphi_{,x}+\psi_{,y})\},$$

$$m_{yy} = -\frac{2}{3}\sigma\kappa_0 h^3\{\kappa_0[(H_{0x}^2 + H_{0z}^2)\Psi_{y,t} - H_{0x}H_{0y}\Psi_{x,t}] - H_{0x}(\varphi_{,x}+\psi_{,y})\}. \tag{41}$$

If eqn (23) is multiplied by dz and integrated from $-h$ to h, taking into account the boundary condition (38), we obtain

$$Q_{x,x} + Q_{y,y} = 2h\rho\Psi_{z,tt} - q. \tag{42}$$

The load q applied to the plate is derived as

$$q = 2h\sigma\kappa_0[H_{0y}\varphi - H_{0x}\psi - \kappa_0(H_{0x}^2 + H_{0y}^2)\Psi_{z,t}]. \tag{43}$$

Substituting eqns (36) and (37) into eqns (39), (40) and (42), we have the equations of motion for a Mindlin plate under the influence of magnetic field

$$\frac{S}{2}[(1-\nu)(\Psi_{x,xx}+\Psi_{x,yy}) + (1+\nu)\Phi_{,x}] - \Psi_x - \Psi_{z,x} = \frac{4h^2\rho}{\pi^2\mu}\Psi_{x,tt} - \frac{6}{\pi^2\mu h}m_{xx}, \tag{44}$$

$$\frac{S}{2}[(1-\nu)(\Psi_{y,xx}+\Psi_{y,yy}) + (1+\nu)\Phi_{,y}] - \Psi_y - \Psi_{z,y} = \frac{4h^2\rho}{\pi^2\mu}\Psi_{y,tt} - \frac{6}{\pi^2\mu h}m_{yy}, \tag{45}$$

$$\Psi_{z,xx} + \Psi_{z,yy} + \Phi = \frac{4h^2\rho}{\pi^2\mu}\frac{1}{R}\Psi_{z,tt} - \frac{6}{\pi^2\mu h}q, \tag{46}$$

in which

$$\Phi = \Psi_{x,x} + \Psi_{y,y}. \tag{47}$$

The rotatory inertia and transverse shear effects are associated with R and S as given by

$$R = \frac{h^2}{3}, \quad S = \frac{6D}{\pi^2 \mu h}. \tag{48}$$

3. PROBLEM STATEMENT AND METHOD OF SOLUTION

Consider an electrically conducting Mindlin plate having a through crack of length $2a$ as shown in Fig. 1. The crack is located on the line $y = 0$, $|x| < a$ and the cracked plate is permeated by the magnetic field $(H_{0y} = H_0, H_{0x} = H_{0z} = 0)$ of magnetic induction $B_0 = \kappa_0 H_0$ normal to the crack surface. Incident waves giving rise to moments symmetric about the crack plane $y = 0$ are applied in an arbitrary direction.

Assuming a quasistatic electromagnetic state which is realized by cancelling the term $f_{,t}$ and retaining other time derivatives in eqns (33)–(35), and neglecting the moments m_{xx} and m_{yy} in eqns (44)–(46), we obtain

$$f_{,x} + \sigma\psi = \frac{h_x(x, y, h, t) - h_x(x, y, -h, t)}{2h}, \tag{49}$$

$$f_{,y} - \sigma(\varphi - \kappa_0 H_0 \Psi_{z,t}) = \frac{h_y(x, y, h, t) - h_y(x, y, -h, t)}{2h}, \tag{50}$$

$$\psi_{,x} - \varphi_{,y} = 0, \tag{51}$$

$$\begin{gathered}
\frac{S}{2}[(1-\nu)(\Psi_{x,xx} + \Psi_{x,yy}) + (1+\nu)\Phi_{,x}] - \Psi_x - \Psi_{z,x} = \frac{4h^2\rho}{\pi^2\mu}\Psi_{x,tt}, \\
\frac{S}{2}[(1-\nu)(\Psi_{y,xx} + \Psi_{y,yy}) + (1+\nu)\Phi_{,y}] - \Psi_y - \Psi_{z,y} = \frac{4h^2\rho}{\pi^2\mu}\Psi_{y,tt}, \\
\Psi_{z,xx} + \Psi_{z,yy} + \Phi = \frac{4h^2\rho}{\pi^2\mu}\frac{1}{R}\Psi_{z,tt} - \frac{12\sigma\kappa_0 H_0}{\pi^2\mu}\varphi + \frac{12\sigma}{\pi^2\mu}(\kappa_0 H_0)^2\Psi_{z,t}.
\end{gathered} \tag{52}$$

The incident waves are expressed as follows:

$$\begin{aligned}
\Psi_x^{i} &= \Psi_{x0}\exp\{-i[k(x\cos\gamma + y\sin\gamma) + \omega t]\}, \\
\Psi_y^{i} &= \Psi_{y0}\exp\{-i[k(x\cos\gamma + y\sin\gamma) + \omega t]\}, \\
\Psi_z^{i} &= \Psi_{z0}\exp\{-i[k(x\cos\gamma + y\sin\gamma) + \omega t]\},
\end{aligned} \tag{53}$$

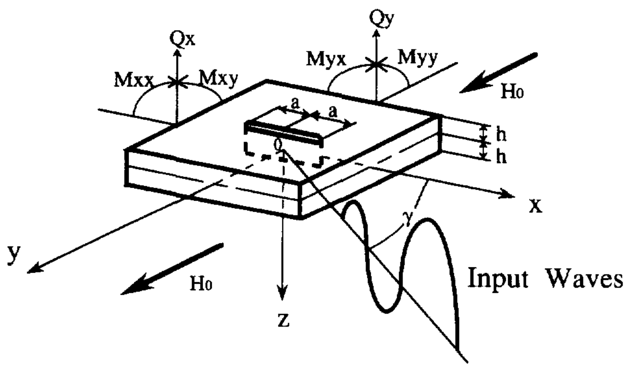

Fig. 1. A through crack in an electrically conducting Mindlin plate and flexural waves.

$$\varphi^{i} = \varphi_0 \exp\{-i[k(x\cos\gamma + y\sin\gamma) + \omega t]\},$$
$$\psi^{i} = \psi_0 \exp\{-i[k(x\cos\gamma + y\sin\gamma) + \omega t]\},$$
$$f^{i} = f_0 \exp\{-i[k(x\cos\gamma + y\sin\gamma) + \omega t]\}, \tag{54}$$

where the superscript i stands for the incident component, $(\Psi_{x0}, \Psi_{y0}, \Psi_{z0}, \varphi_0, \psi_0, f_0)$ are the amplitudes of the input waves $(\Psi^{i}_{x}, \Psi^{i}_{y}, \Psi^{i}_{z}, \varphi^{i}, \psi^{i}, f^{i})$, k is the wave number and ω is the circular frequency. The angle of incidence γ lies between the limits $-\pi$ and π and is measured from the positive x-axis. The field eqns (10) and (11) in the vacuum can be written as

$$h^{e}_{z,y} - h^{e}_{y,z} = 0,$$
$$h^{e}_{x,z} - h^{e}_{z,x} = 0,$$
$$h^{e}_{y,x} - h^{e}_{x,y} = 0, \tag{55}$$

$$h^{e}_{x,x} + h^{e}_{y,y} + h^{e}_{z,z} = 0. \tag{56}$$

Outside the plate the external fields are solutions of eqns (55) and (56). Solutions of these equations which vanish at $z = \pm\infty$ and have the wave factor $\exp[-i\{k(x\cos\gamma + y\sin\gamma) + \omega t\}]$ are

$$h^{ei}_{x} = i\cos\gamma A_0 \exp(-kz)\exp\{-i[k(x\cos\gamma + y\sin\gamma) + \omega t]\} \quad (z \geqslant h),$$
$$= -i\cos\gamma A_0 \exp(kz)\exp\{-i[k(x\cos\gamma + y\sin\gamma) + \omega t]\} \quad (z \leqslant -h),$$
$$h^{ei}_{y} = i\sin\gamma A_0 \exp(-kz)\exp\{-i[k(x\cos\gamma + y\sin\gamma) + \omega t]\} \quad (z \geqslant h),$$
$$= -i\sin\gamma A_0 \exp(kz)\exp\{-i[k(x\cos\gamma + y\sin\gamma) + \omega t]\} \quad (z \leqslant -h),$$
$$h^{ei}_{z} = A_0 \exp(-kz)\exp\{-i[k(x\cos\gamma + y\sin\gamma) + \omega t]\} \quad (z \geqslant h),$$
$$= A_0 \exp(kz)\exp\{-i[k(x\cos\gamma + y\sin\gamma) + \omega t]\} \quad (z \leqslant -h), \tag{57}$$

where A_0 is an undetermined constant.

Making use of eqns (57) and (29) renders the x, y-magnetic intensity components $h^{i}_{x}(x, y, \pm h, t)$, $h^{i}_{y}(x, y, \pm h, t)$ and the amplitude f_0

$$h^{i}_{x}(x, y, \pm h, t) = \pm i\cos\gamma f_0 \exp\{-i[k(x\cos\gamma + y\sin\gamma) + \omega t]\},$$
$$h^{i}_{y}(x, y, \pm h, t) = \pm i\sin\gamma f_0 \exp\{-i[k(x\cos\gamma + y\sin\gamma) + \omega t]\},$$
$$f_0 = A_0 \exp(-kh). \tag{58}$$

Substituting eqns (53), (54) and (58) into eqns (49)–(51), we obtain

$$(kh+1)\cos\gamma f_0 + i\sigma h\psi_0 = 0, \quad \varphi_0 = -i\omega\kappa_0 H_0 \cos^2\gamma\Psi_{z0}, \quad \sin\gamma\varphi_0 = \cos\gamma\psi_0. \tag{59}$$

Substituting eqns (53) and (54) into eqns (52) yields

$$\begin{vmatrix} d_{11} & d_{12} & d_{13} \\ d_{21} & d_{22} & d_{23} \\ d_{31} & d_{32} & d_{33} \end{vmatrix} = 0, \tag{60}$$

$$i\frac{\pi^2}{6}kh\Psi_{x0} = -\cos\gamma\left[\frac{\pi^2}{6}kh - 2kh\left(\frac{\omega}{kc_2}\right)^2 - 2i\left(\frac{\omega}{kc_2}\right)\Gamma_h\sin^2\gamma\right]k\Psi_{z0},$$

$$i\frac{\pi^2}{6}kh\Psi_{y0} = -\sin\gamma\left[\frac{\pi^2}{6}kh - 2kh\left(\frac{\omega}{kc_2}\right)^2 - 2i\left(\frac{\omega}{kc_2}\right)\Gamma_h\sin^2\gamma\right]k\Psi_{z0}, \tag{61}$$

in which $c_2 = (\mu/\rho)^{1/2}$ is the shear wave velocity and

$$d_{11} = \frac{4(kh)^2}{3(1-\nu)}\left(\frac{1-\nu}{2}\sin^2\gamma + \cos^2\gamma\right) + \frac{\pi^2}{6} - \frac{2}{3}(kh)^2\left(\frac{\omega}{kc_2}\right)^2,$$

$$d_{12} = d_{21} = \frac{2(1+\nu)}{3(1-\nu)}(kh)^2\sin\gamma\cos\gamma,$$

$$d_{13} = -d_{31} = -i\frac{\pi^2}{6}kh\cos\gamma,$$

$$d_{22} = \frac{4(kh)^2}{3(1-\nu)}\left(\sin^2\gamma + \frac{1-\nu}{2}\cos^2\gamma\right) + \frac{\pi^2}{6} - \frac{2}{3}(kh)^2\left(\frac{\omega}{kc_2}\right)^2,$$

$$d_{23} = -d_{32} = -i\frac{\pi^2}{6}kh\sin\gamma,$$

$$d_{33} = \frac{\pi^2}{6}(kh)^2 - 2(kh)^2\left(\frac{\omega}{kc_2}\right)^2 - 2ikh\left(\frac{\omega}{kc_2}\right)\Gamma_h\sin^2\gamma, \tag{62}$$

$$\Gamma_h = h_c\sigma_h,$$

$$h_c = \frac{\kappa_0 H_0^2}{\mu},$$

$$\sigma_h = c_2 h\sigma\kappa_0. \tag{63}$$

The effect of the magnetic field ($H_{0y} = H_0, H_{0x} = H_{0z} = 0$) on the flexural waves at $\gamma = \pi/2$ is discussed in Appendix A and the assumption of a quasistatic electromagnetic state is justified. The dependency of the flexural waves on kh for three directions of the magnetic field ($H_{0x} = H_0, H_{0y} = H_{0z} = 0; H_{0y} = H_0, H_{0x} = H_{0z} = 0; H_{0z} = H_0, H_{0x} = H_{0y} = 0$) is discussed in Appendix B.

The complete solution of the waves as diffracted by the crack is obtained by adding the incident and scattered waves, i.e.,

$$\Psi_x(x,y,t) = \Psi_x^{i}(x,y,t) + \Psi_x^{s}(x,y,t),$$

$$\Psi_y(x,y,t) = \Psi_y^{i}(x,y,t) + \Psi_y^{s}(x,y,t),$$

$$\Psi_z(x,y,t) = \Psi_z^{i}(x,y,t) + \Psi_z^{s}(x,y,t),$$

$$\varphi(x,y,t) = \varphi^{i}(x,y,t) + \varphi^{s}(x,y,t),$$

$$\psi(x,y,t) = \psi^{i}(x,y,t) + \psi^{s}(x,y,t),$$

$$f(x,y,t) = f^{i}(x,y,t) + f^{s}(x,y,t), \tag{64}$$

where the superscript s stands for the scattered component. Likewise, the plate displacements, moments and shears can also be found by superposing the incident and scattered parts and the results are obvious. For a traction-free crack, the quantities M_{yy}, M_{xy}, Q_y must each vanish for $|x| < a$ and $y = 0$. The boundary conditions for the scattered field become

$$M^s_{xy} = 0 \quad (y = 0, 0 \leqslant |x| < \infty), \tag{65}$$

$$Q^s_y = 0 \quad (y = 0, 0 \leqslant |x| < \infty), \tag{66}$$

$$e^s_y = 0 \quad (y = 0, 0 \leqslant |x| < \infty), \tag{67}$$

$$\begin{cases} M^s_{yy} = -M^i_{yy} & (y = 0, 0 \leqslant |x| < a), \\ \Psi^s_y = 0 & (y = 0, a \leqslant |x| < \infty), \end{cases} \tag{68}$$

in which

$$M^i_{yy} = -ikD\Psi_0(\sin^2\gamma + v\cos^2\gamma)\exp[-i(kx\cos\gamma + \omega t)], \tag{69}$$

$$\Psi_0 = \frac{1}{\cos\gamma}\Psi_{x0} = \frac{1}{\sin\gamma}\Psi_{y0}. \tag{70}$$

In what follows, the exponential time factor $\exp(-i\omega t)$ would be omitted as it always appears with the quantity $ikD\Psi_0(\sin^2\gamma + v\cos^2\gamma)\exp(-ikx\cos\gamma)$ as indicated in eqn (69).

We assume that the solutions Ψ_x, Ψ_y, Ψ_z, φ, ψ and f are of the forms

$$\Psi_x(x, y) = \frac{1}{\pi}\sum_{j=1}^{3}\int_{-\infty}^{\infty} A_j(\alpha)\exp[-\gamma_j(\alpha)y]\exp(-i\alpha x)\,d\alpha,$$

$$\Psi_y(x, y) = \frac{1}{\pi}\sum_{j=1}^{3}\int_{-\infty}^{\infty} B_j(\alpha)\exp[-\gamma_j(\alpha)y]\exp(-i\alpha x)\,d\alpha,$$

$$\Psi_z(x, y) = \frac{1}{\pi}\sum_{j=1}^{3}\int_{-\infty}^{\infty} C_j(\alpha)\exp[-\gamma_j(\alpha)y]\exp(-i\alpha x)\,d\alpha, \tag{71}$$

$$\varphi(x, y) = \frac{1}{\pi}\sum_{j=1}^{3}\int_{-\infty}^{\infty} D_j(\alpha)\exp[-\gamma_j(\alpha)y]\exp(-i\alpha x)\,d\alpha,$$

$$\psi(x, y) = \frac{1}{\pi}\sum_{j=1}^{3}\int_{-\infty}^{\infty} E_j(\alpha)\exp[-\gamma_j(\alpha)y]\exp(-i\alpha x)\,d\alpha,$$

$$f(x, y) = \frac{1}{\pi}\sum_{j=1}^{3}\int_{-\infty}^{\infty} F_j(\alpha)\exp[-\gamma_j(\alpha)y]\exp(-i\alpha x)\,d\alpha, \tag{72}$$

where $A_j(\alpha)$, $B_j(\alpha)$, $C_j(\alpha)$, $D_j(\alpha)$, $E_j(\alpha)$, $F_j(\alpha)$ and $\gamma_j(\alpha)$ $(j = 1, 2, 3)$ are the unknown functions of the transform variable α to be determined later. It can be shown that the solutions (h^e_x, h^e_y, h^e_z) satisfying eqns (55) and (56) are given by

$$h^e_x = i\frac{1}{\pi}\sum_{j=1}^{3}\int_{-\infty}^{\infty}\frac{\alpha}{[\alpha^2 - \gamma_j^2(\alpha)]^{1/2}}a_{1j}(\alpha)\exp[-\gamma_j(\alpha)y]\exp\{-[\alpha^2 - \gamma_j^2(\alpha)]^{1/2}z\}\exp(-i\alpha x)\,d\alpha$$

$$(z \geqslant h)$$

$$= -i\frac{1}{\pi}\sum_{j=1}^{3}\int_{-\infty}^{\infty}\frac{\alpha}{[\alpha^2-\gamma_j^2(\alpha)]^{1/2}}a_{2j}(\alpha)\exp[-\gamma_j(\alpha)y]\exp\{[\alpha^2-\gamma_j^2(\alpha)]^{1/2}z\}\exp(-i\alpha x)\,d\alpha$$

$$(z \leqslant -h), \quad (73)$$

$$h_y^e = \frac{1}{\pi}\sum_{j=1}^{3}\int_{-\infty}^{\infty}\frac{\gamma_j(\alpha)}{[\alpha^2-\gamma_j^2(\alpha)]^{1/2}}a_{1j}(\alpha)\exp[-\gamma_j(\alpha)y]\exp\{-[\alpha^2-\gamma_j^2(\alpha)]^{1/2}z\}\exp(-i\alpha x)\,d\alpha$$

$$(z \geqslant h)$$

$$= -\frac{1}{\pi}\sum_{j=1}^{3}\int_{-\infty}^{\infty}\frac{\gamma_j(\alpha)}{[\alpha^2-\gamma_j^2(\alpha)]^{1/2}}a_{2j}(\alpha)\exp[-\gamma_j(\alpha)y]\exp\{[\alpha^2-\gamma_j^2(\alpha)]^{1/2}z\}\exp(-i\alpha x)\,d\alpha$$

$$(z \leqslant -h), \quad (74)$$

$$h_z^e = \frac{1}{\pi}\sum_{j=1}^{3}\int_{-\infty}^{\infty}a_{1j}(\alpha)\exp[-\gamma_j(\alpha)y]\exp\{-[\alpha^2-\gamma_j^2(\alpha)]^{1/2}z\}\exp(-i\alpha x)\,d\alpha$$

$$(z \geqslant h)$$

$$= \frac{1}{\pi}\sum_{j=1}^{3}\int_{-\infty}^{\infty}a_{2j}(\alpha)\exp[-\gamma_j(\alpha)y]\exp\{[\alpha^2-\gamma_j^2(\alpha)]^{1/2}z\}\exp(-i\alpha x)\,d\alpha$$

$$(z \leqslant -h), \quad (75)$$

where the unknowns $a_{1j}(\alpha)$ and $a_{2j}(\alpha)$ $(j = 1, 2, 3)$ are to be evaluated from the boundary conditions (29) at $|z| = h$.

Making use of eqns (73)–(75) and (29) renders the magnetic intensity components $h_x(x, y, \pm h, t)$, $h_y(x, y, \pm h, t)$ and the unknown function $F_j(\alpha)$

$$h_x(x, y, \pm h, t) = \pm i\frac{1}{\pi}\sum_{j=1}^{3}\int_{-\infty}^{\infty}\frac{\alpha}{[\alpha^2-\gamma_j^2(\alpha)]^{1/2}}a_{1j}(\alpha)\exp[-\gamma_j(\alpha)y]$$
$$\times\exp\{-[\alpha^2-\gamma_j^2(\alpha)]^{1/2}h\}\exp(-i\alpha x)\,d\alpha,$$

$$h_y(x, y, \pm h, t) = \pm\frac{1}{\pi}\sum_{j=1}^{3}\int_{-\infty}^{\infty}\frac{\gamma_j(\alpha)}{[\alpha^2-\gamma_j^2(\alpha)]^{1/2}}a_{1j}(\alpha)\exp[-\gamma_j(\alpha)y]$$
$$\times\exp\{-[\alpha^2-\gamma_j^2(\alpha)]^{1/2}h\}\exp(-i\alpha x)\,d\alpha,$$

$$F_j(\alpha) = a_{1j}(\alpha)\exp\{-[\alpha^2-\gamma_j^2(\alpha)]^{1/2}h\}. \quad (76)$$

Substituting eqns (71), (72) and (76) into eqns (49)–(51), we have

$$\left\{h+\frac{1}{[\alpha^2-\gamma_j^2(\alpha)]^{1/2}}\right\}\alpha F_j(\alpha)+i\sigma hE_j(\alpha) = 0 \quad (j = 1, 2, 3),$$

$$[\alpha^2-\gamma_j^2(\alpha)]D_j(\alpha) = -i\omega\kappa_0 H_0\alpha^2 C_j(\alpha) \quad (j = 1, 2, 3),$$

$$i\alpha E_j(\alpha) = \gamma_j(\alpha)D_j(\alpha) \quad (j = 1, 2, 3). \quad (77)$$

Substituting eqns (71) and (72) into eqns (52) yields

$$\gamma_j^6(\alpha)+a_0(\alpha)\gamma_j^4(\alpha)+b_0(\alpha)\gamma_j^2(\alpha)+c_0(\alpha) = 0, \quad (78)$$

$$[\alpha^2-\gamma_j^2(\alpha)]A_j(\alpha) = i\alpha G_j(\alpha)C_j(\alpha) \quad (j = 1, 2, 3),$$

$$[\alpha^2-\gamma_j^2(\alpha)]B_j(\alpha) = \gamma_j(\alpha)G_j(\alpha)C_j(\alpha) \quad (j = 1,2,3), \tag{79}$$

in which

$$\begin{aligned} a_0(\alpha) &= -3\alpha^2+\left(\frac{\omega}{\omega_0}\right)^2\left(\frac{1}{S}+\frac{1}{R}\right)+i\omega\frac{12\sigma\kappa_0 h_c}{\pi^2}, \\ b_0(\alpha) &= 3\alpha^4-2\alpha^2\left(\frac{\omega}{\omega_0}\right)^2\left(\frac{1}{S}+\frac{1}{R}\right)-\alpha^2 i\omega\frac{12\sigma\kappa_0 h_c}{\pi^2} \\ &\quad +\frac{1}{RS}\left(\frac{\omega}{\omega_0}\right)^2\left[\left(\frac{\omega}{\omega_0}\right)^2-1\right]+\frac{1}{S}\left[\left(\frac{\omega}{\omega_0}\right)^2-1\right]i\omega\frac{12\sigma\kappa_0 h_c}{\pi^2}, \\ c_0(\alpha) &= -\alpha^6+\alpha^4\left(\frac{\omega}{\omega_0}\right)^2\left(\frac{1}{S}+\frac{1}{R}\right)-\alpha^2\frac{1}{RS}\left(\frac{\omega}{\omega_0}\right)^2\left[\left(\frac{\omega}{\omega_0}\right)^2-1\right], \end{aligned} \tag{80}$$

$$G_j(\alpha) = \alpha^2-\gamma_j^2(\alpha)-\left(\frac{\omega}{\omega_0}\right)^2\frac{1}{R}+i\omega\frac{12\sigma\kappa_0 h_c}{\pi^2}\frac{\gamma_j^2(\alpha)}{\alpha^2-\gamma_j^2(\alpha)} \quad (j = 1,2,3), \tag{81}$$

and $\omega_0 = \pi c_2/2h$ is the cut-off frequency. Substituting eqns (71) into eqns (52), taking into account eqns (79), we obtain $\varphi(x,y)$ as

$$\varphi(x,y) = \frac{-i\omega\kappa_0 H_0}{d_0}\frac{1}{\pi}\sum_{j=1}^{3}\int_{-\infty}^{\infty} H_j(\alpha)C_j(\alpha)\exp[-\gamma_j(\alpha)y]\exp(-i\alpha x)\,\mathrm{d}\alpha, \tag{82}$$

in which

$$\begin{aligned} d_0 &= \frac{1}{S}\left[\left(\frac{\omega}{\omega_0}\right)^2-1\right]i\omega\frac{12\sigma\kappa_0 h_c}{\pi^2}, \\ H_j(\alpha) &= \gamma_j^4(\alpha)+M_1(\alpha)\gamma_j^2(\alpha)+M_2(\alpha) \quad (j = 1,2,3), \\ M_1(\alpha) &= -2\alpha^2+\left(\frac{\omega}{\omega_0}\right)^2\left(\frac{1}{S}+\frac{1}{R}\right)+i\omega\frac{12\sigma\kappa_0 h_c}{\pi^2}, \\ M_2(\alpha) &= \alpha^4-\alpha^2\left(\frac{\omega}{\omega_0}\right)^2\left(\frac{1}{S}+\frac{1}{R}\right)+\frac{1}{RS}\left(\frac{\omega}{\omega_0}\right)^2\left[\left(\frac{\omega}{\omega_0}\right)^2-1\right] \\ &\quad +\frac{1}{S}\left[\left(\frac{\omega}{\omega_0}\right)^2-1\right]i\omega\frac{12\sigma\kappa_0 h_c}{\pi^2}. \end{aligned} \tag{83}$$

From eqns (51) and (82), we also obtain $\psi(x,y)$ as

$$\psi(x,y) = \frac{-\omega\kappa_0 H_0}{d_0}\frac{1}{\pi}\sum_{j=1}^{3}\int_{-\infty}^{\infty}\frac{T_j(\alpha)}{\alpha}C_j(\alpha)\exp[-\gamma_j(\alpha)y]\exp(-i\alpha x)\,\mathrm{d}\alpha, \tag{84}$$

in which

$$T_j(\alpha) = [\gamma_j^4(\alpha)+M_1(\alpha)\gamma_j^2(\alpha)+M_2(\alpha)]\gamma_j(\alpha) \quad (j = 1,2,3). \tag{85}$$

The boundary conditions (65)–(67) render

$$\sum_{j=1}^{3} R_j(\alpha)C_j(\alpha) = 0, \tag{86}$$

$$\sum_{j=1}^{3} [P_j(\alpha)-\gamma_j(\alpha)]C_j(\alpha) = 0, \tag{87}$$

$$\sum_{j=1}^{3} T_j(\alpha)C_j(\alpha) = 0, \tag{88}$$

in which

$$R_j(\alpha) = -N_j(\alpha)\gamma_j(\alpha)-\alpha P_j(\alpha) \quad (j = 1,2,3), \tag{89}$$

$$N_j(\alpha) = -\frac{\alpha L_j(\alpha)}{\gamma_j^2(\alpha)-\alpha^2} \quad (j = 1,2,3), \tag{90}$$

$$P_j(\alpha) = -\frac{\gamma_j(\alpha)L_j(\alpha)}{\gamma_j^2(\alpha)-\alpha^2} \quad (j = 1,2,3), \tag{91}$$

$$L_j(\alpha) = \alpha^2-\gamma_j^2(\alpha)+i\omega\frac{12\sigma\kappa_0 h_c}{\pi^2}\frac{1}{d_0}[\gamma_j^4(\alpha)+M_1(\alpha)\gamma_j^2(\alpha)+M_2(\alpha)] -\left(\frac{\omega}{\omega_0}\right)^2\frac{1}{R}-i\omega\frac{12\sigma\kappa_0 h_c}{\pi^2} \quad (j = 1,2,3). \tag{92}$$

Let $C(\alpha)$ be defined as

$$C(\alpha) = \sum_{j=1}^{3} P_j(\alpha)C_j(\alpha). \tag{93}$$

Application of the boundary conditions (68) gives rise to a pair of dual integral equations:

$$\begin{cases} \int_{-\infty}^{\infty} \alpha f(\alpha)C(\alpha)\exp(-i\alpha x)\,d\alpha = \frac{\pi M_{iy}}{D}(\sin^2\gamma+\nu\cos^2\gamma)\exp(-ikx\cos\gamma) & (0 \leqslant |x| < a), \\ \int_{-\infty}^{\infty} C(\alpha)\exp(-i\alpha x)\,d\alpha = 0 & (a \leqslant |x| < \infty), \end{cases} \tag{94}$$

in which M_{iy} and $f(\alpha)$ are known as

$$M_{iy} = ikD\Psi_0, \tag{95}$$

$$f(\alpha) = \frac{1}{\alpha U(\alpha)}[V_1(\alpha)-G(\alpha)V_2(\alpha)-H(\alpha)V_3(\alpha)], \tag{96}$$

$$U(\alpha) = P_1(\alpha)-P_2(\alpha)G(\alpha)-P_3(\alpha)H(\alpha), \tag{97}$$

$$G(\alpha) = \frac{S_1(\alpha)T_3(\alpha)-S_3(\alpha)T_1(\alpha)}{S_2(\alpha)T_3(\alpha)-S_3(\alpha)T_2(\alpha)}, \tag{98}$$

$$H(\alpha) = \frac{S_1(\alpha)T_2(\alpha) - S_2(\alpha)T_1(\alpha)}{S_3(\alpha)T_2(\alpha) - S_2(\alpha)T_3(\alpha)}, \tag{99}$$

$$S_j(\alpha) = P_j(\alpha) - \gamma_j(\alpha) \quad (j = 1, 2, 3), \tag{100}$$

$$V_j(\alpha) = -P_j(\alpha)\gamma_j(\alpha) + \nu\alpha N_j(\alpha) \quad (j = 1, 2, 3). \tag{101}$$

The second of eqns (94) would be satisfied if $C(\alpha)$ is taken as

$$C(\alpha) = \frac{\pi M_{iy}}{DF}(\sin^2\gamma + \nu\cos^2\gamma)a^2\left[\int_0^1 \xi^{1/2}\Phi_2(\xi)J_0(a\alpha\xi)\,d\xi + \int_0^1 \xi^{1/2}\Psi_2(\xi)J_1(a\alpha\xi)\,d\xi\right], \tag{102}$$

where $J_0()$ and $J_1()$ being the first kind Bessel functions of order zero and one, and

$$F = \lim_{\alpha\to\infty} f(\alpha). \tag{103}$$

Inserting eqn (102) into the first of eqns (94) yields the Fredholm integral equations of the second kind:

$$\Phi_2(\xi) + \int_0^1 K_1(\xi,\eta)\Phi_2(\eta)\,d\eta = \xi^{1/2}J_0(ka\xi\cos\gamma), \tag{104}$$

$$\Psi_2(\xi) + \int_0^1 K_2(\xi,\eta)\Psi_2(\eta)\,d\eta = \xi^{1/2}J_1(ka\xi\cos\gamma), \tag{105}$$

where the kernels $K_1(\xi,\eta)$ and $K_2(\xi,\eta)$ are given by

$$K_1(\xi,\eta) = (\xi\eta)^{1/2}\int_0^\infty \alpha\left[\frac{1}{F}f(\alpha/a) - 1\right]J_0(\alpha\xi)J_0(\alpha\eta)\,d\alpha, \tag{106}$$

$$K_2(\xi,\eta) = (\xi\eta)^{1/2}\int_0^\infty \alpha\left[\frac{1}{F}f(\alpha/a) - 1\right]J_1(\alpha\xi)J_1(\alpha\eta)\,d\alpha. \tag{107}$$

The moment intensity factor is defined by

$$\begin{aligned} K_1 &= \lim_{x\to a^+}[2\pi(x-a)]^{1/2}M_{yy}(x,0) \\ &= M_0\left(\frac{k}{k_1}\right)(\pi a)^{1/2}(\sin^2\gamma + \nu\cos^2\gamma)[\Phi_2(1) - i\Psi_2(1)] \\ &= M_0M_2(\pi a)^{1/2}(\sin^2\gamma + \nu\cos^2\gamma)[\Phi_2(1) - i\Psi_2(1)], \end{aligned} \tag{108}$$

in which

$$M_0 = ik_1D\Psi_0,$$

$$M_2 = \frac{k}{k_1},$$

$$k_1^2 = \frac{1}{2}\left(\frac{\omega}{\omega_0}\right)^2 \left\{\frac{1}{S} + \frac{1}{R} + \left[\left(\frac{1}{S} - \frac{1}{R}\right)^2 + \frac{4}{RS}\left(\frac{\omega_0}{\omega}\right)^2\right]^{1/2}\right\}. \tag{109}$$

Keep in mind that the factor $\exp(-i\omega t)$ has been suppressed.

4. DISCUSSION OF RESULTS

The elastodynamic plate solution Ref. [7] is recovered when the magnetic field tends to zero. In the limit as $\omega \to 0$ at $\gamma = \pi/2$, the corresponding static solution of $K_1 = M_0(\pi a)^{1/2}$ is obtained. The considered conductor is graphite. The material properties are given in Table 1. Computed are the numerical values of $\Phi_2(1)$ and $\Psi_2(1)$ in eqns (104) and (105) for $v = 0.3$. The ratio k/k_1 in eqn (108) is known from ω in eqn (60) which can be further reduced to

$$\left(\frac{k}{k_1}\right)^6 + a_1\left(\frac{k}{k_1}\right)^4 + b_1\left(\frac{k}{k_1}\right)^2 + c_1 = 0, \tag{110}$$

in which

$$a_1 = \frac{2}{(1-v)k_1^2}\left\{\frac{1}{S}\left[1 - \frac{3-v}{2}\left(\frac{\omega}{\omega_0}\right)^2\right] - \frac{1-v}{2R}\left[\left(\frac{\omega}{\omega_0}\right)^2 + i\frac{2}{\pi}\left(\frac{\omega}{\omega_0}\right)\Gamma_h \sin^2\gamma\right]\right\},$$

$$b_1 = \frac{2}{(1-v)k_1^4}\left[1 - \left(\frac{\omega}{\omega_0}\right)^2\right]\left\{\frac{1}{S^2}\left[1 - \left(\frac{\omega}{\omega_0}\right)^2\right] - \frac{3-v}{2SR}\left[\left(\frac{\omega}{\omega_0}\right)^2 + i\frac{2}{\pi}\left(\frac{\omega}{\omega_0}\right)\Gamma_h \sin^2\gamma\right]\right\},$$

$$c_1 = \frac{2}{(1-v)S^2Rk_1^6}\left[1 - \left(\frac{\omega}{\omega_0}\right)^2\right]\left[\left(\frac{\omega}{\omega_0}\right)^2 + i\frac{2}{\pi}\left(\frac{\omega}{\omega_0}\right)\Gamma_h \sin^2\gamma\right]. \tag{111}$$

The normalized magnetic field of $\Gamma_h = 0.0$, 0.01, 0.02 and 0.03 ($\sigma_h = 0.5$) correspond, respectively, to magnetic induction $B_0 = \kappa_0 H_0 = 0.0$, 7.0, 9.9 and 12.2 T (tesla).

Figure 2 shows a plot of the normalized moment intensity factor $|K_1/M_0(\pi a)^{1/2}|$ vs frequency ω normalized against the cut-off frequency ω_0 for flexural waves at normal incidence, i.e. $\gamma = \pi/2$, the ratio $a/h = 5$ and four different values of Γ_h mentioned earlier. The dashed curve obtained for the case of $\Gamma_h = 0.0$ coincides with the purely elastic case. The quantity $|K_1/M_0(\pi a)^{1/2}|$ for $\Gamma_h = 0.0$ is found to be smaller than the static case and decrease in magnitude as the frequency is increased. As the three curves for $\Gamma_h \neq 0.0$ possess higher amplitude than that for $\Gamma_h = 0.0$, the magnetic field is seen to increase the local moment with increasing Γ_h. Such an effect dies out at high frequency. The magnetic field effect for $\Gamma_h = 0.01$, 0.02, 0.03 can increase $|K_1/M_0(\pi a)^{1/2}|$ by approximately 25.1, 60.1, 91.3% for $\omega/\omega_0 = 0.005$ and 6.9, 23.1, 40.4% for $\omega/\omega_0 = 0.01$ over the corresponding value for the purely elastic case, respectively. Figures 3–6 show the corresponding results for $\gamma = \pi/6$, $\pi/3$, $2\pi/3$ and $5\pi/6$. The same gross effect is observed. If ω/ω_0 is held constant, increasing Γ_h increases the dynamic moment intensity factor depending on γ. Figure 7 shows the effect of $\Gamma_h = 0.03$ on the variations of $|K_1/M_0(\pi a)^{1/2}|$ for $\gamma = \pi/4$, $\pi/2$ and $a/h = 5$. The effect of $\Gamma_h = 0.03$ on the normalized moment intensity factor $|K_1/M_0(\pi a)^{1/2}|$ for $\gamma = \pi/2$ is larger than that for $\gamma = \pi/4$. A typical set of parametric curves for $\omega/\omega_0 = 0.01$ and

Table 1. Material properties of graphite

Material	Density ρ (kg/m^3)	Electrical conductivity σ (mho/m)	Shear modulus μ (N/m^2)
Graphite	2250	1.25×10^5	1.96×10^9

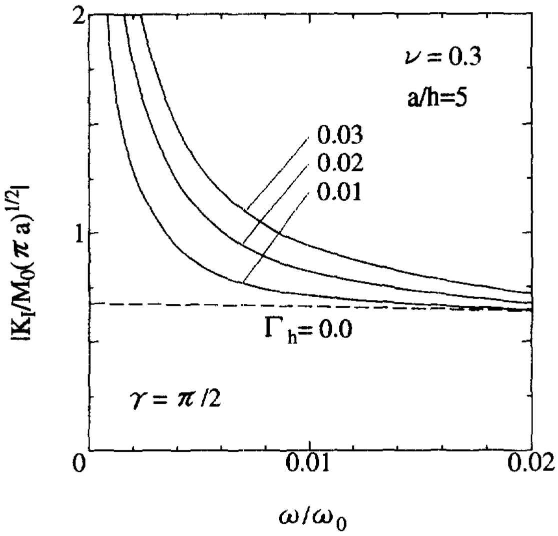

Fig. 2. Dynamic bending moment intensity factor $|K_I/M_0(\pi a)^{1/2}|$ vs ω/ω_0 ($\gamma = \pi/2, a/h = 5$).

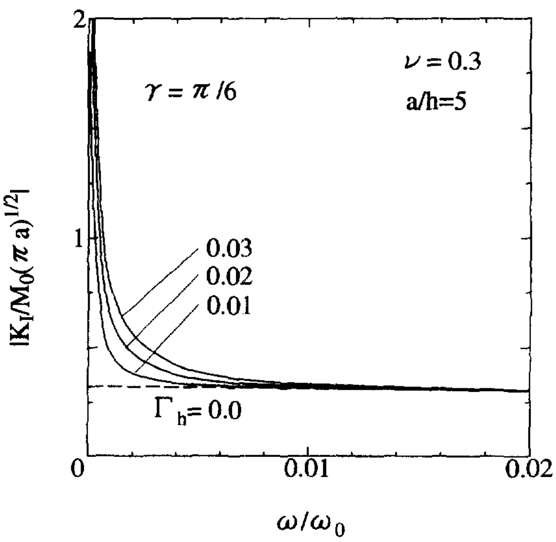

Fig. 3. Dynamic bending moment intensity factor $|K_I/M_0(\pi a)^{1/2}|$ vs ω/ω_0 ($\gamma = \pi/6, a/h = 5$).

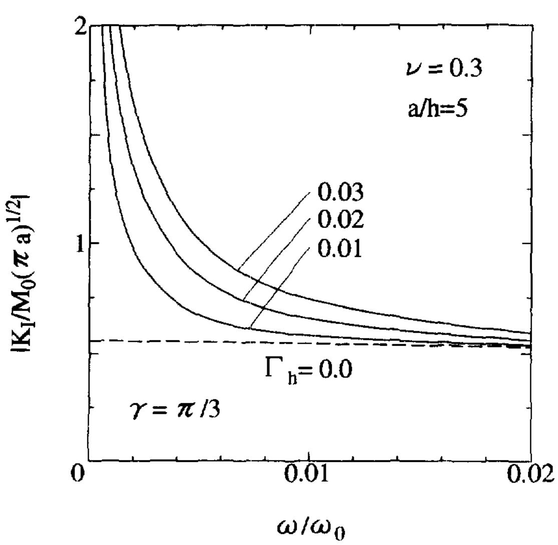

Fig. 4. Dynamic bending moment intensity factor $|K_I/M_0(\pi a)^{1/2}|$ vs ω/ω_0 ($\gamma = \pi/3, a/h = 5$).

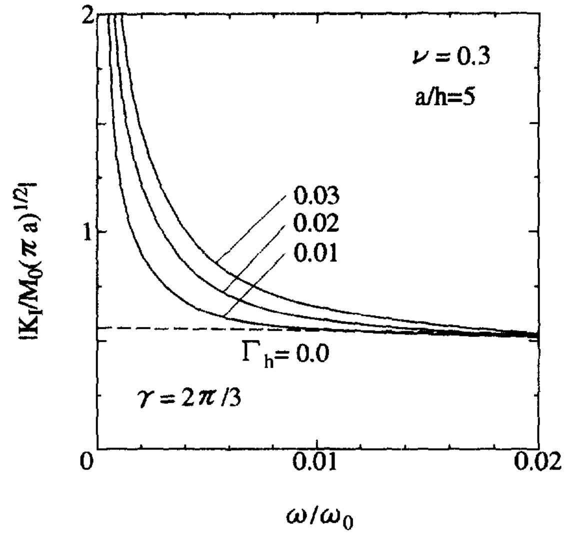

Fig. 5. Dynamic bending moment intensity factor $|K_I/M_0(\pi a)^{1/2}|$ vs ω/ω_0 ($\gamma = 2\pi/3, a/h = 5$).

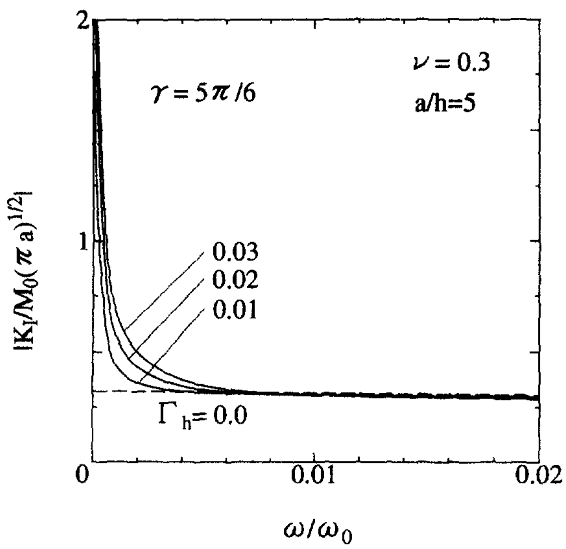

Fig. 6. Dynamic bending moment intensity factor $|K_I/M_0(\pi a)^{1/2}|$ vs ω/ω_0 ($\gamma = 5\pi/6, a/h = 5$).

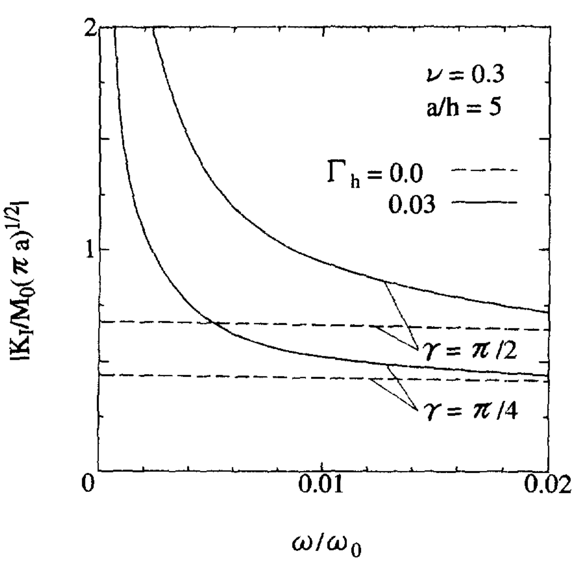

Fig. 7. Dynamic bending moment intensity factor $|K_I/M_0(\pi a)^{1/2}|$ vs ω/ω_0 ($a/h = 5$).

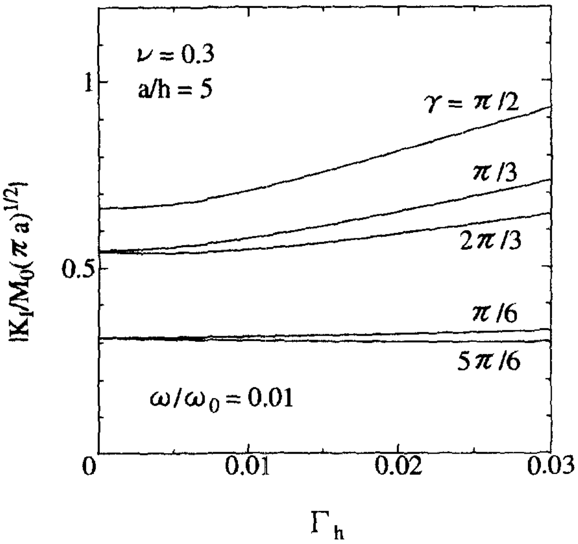

Fig. 8. Dynamic bending moment intensity factor $|K_I/M_0(\pi a)^{1/2}|$ vs Γ_h ($\omega/\omega_0 = 0.01, a/h = 5$).

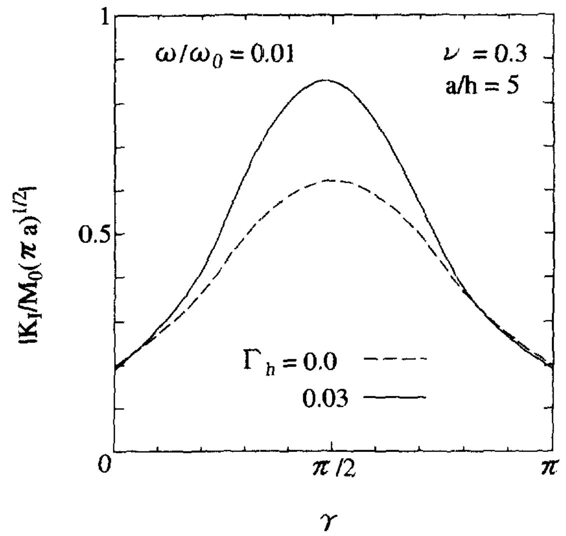

Fig. 9. Dynamic bending moment intensity factor $|K_I/M_0(\pi a)^{1/2}|$ vs γ ($\omega/\omega_0 = 0.01, a/h = 5$).

$a/h = 5$ is given in Fig. 8 to illustrate the variation of $|K_I/M_0(\pi a)^{1/2}|$ with Γ_h. Note that $|K_I/M_0(\pi a)^{1/2}|$ approaches 0.661 as $\omega/\omega_0 \to 0$ at $\Gamma_h = 0.0$ and $\gamma = \pi/2$, and tends to increase with increasing Γ_h, depending on γ. For $\nu = 0.3$, $a/h = 5$ and $\omega/\omega_0 = 0.01$, it is observed that the magnetic field effect of $\Gamma_h = 0.03$ can increase $|K_I/M_0(\pi a)^{1/2}|$ by approximately 40.4% ($\gamma = \pi/2$), 34.8, 19.7% ($\gamma = \pi/3, 2\pi/3$), and 5.6, -3.3% ($\gamma = \pi/6, 5\pi/6$), respectively. Figure 9 shows the dependency of $|K_I/M_0(\pi a)^{1/2}|$ on γ for $\omega/\omega_0 = 0.01$, $\Gamma_h = 0, 0.03$, and $a/h = 5$. The effect of the magnetic field on $|K_I/M_0(\pi a)^{1/2}|$ for $\gamma = \pi/2$ is more pronounced than that for $\gamma \neq \pi/2$.

In conclusion, the magneto-elastic analysis of a conducting Mindlin plate with a through crack subjected to a steady-state magnetic field normal to the crack and an incident oblique flexural wave has been shown in this study. Mindlin's theory of plate bending including dynamic magneto-elastic effects is applied and the results are expressed in terms of the bending moment intensity factor. A quasistatic electromagnetic field is assumed for the plate. The dynamic moment intensity factor decreases with the increase of the frequency of the input wave ω depending on the angle of incidence γ, the crack length to the plate-thickness ratio a/h, the Poisson's ratio ν and the magnetic field Γ_h. The existence of the magnetic field produces larger values of the dynamic moment intensity factor. A significant increase in the local moment intensity factor occurs at wave frequency $\omega/\omega_0 < 0.02$ and normal incidence $\gamma = \pi/2$, and the magnetic field effect dies out gradually as the frequency is increased.

REFERENCES

Ambartsumian, S. A., Bagdasarian, G. E. and Belubekian, M. V. (1971) On the three-dimensional problem of magnetoelastic plate vibrations. *Journal of Applied Mathematics and Mechanics (PMM)* **35,** 184–195.

Ambartsumian, S. A., Bagdasarian, G. E. and Belubekian, M. V. (1975) On the equations of magnetoelastic thin plate. *Journal of Applied Mathematics and Mechanics (PMM)* **39,** 922–926.

Dunkin, J. W. and Eringen, A. C. (1963) On the propagation of waves in an electromagnetic elastic solid. *International Journal of Engineering Science* **1,** 461–495.

Mindlin, R. D. (1951) Influence of rotatory inertia and shear on flexural motions of isotropic, elastic plates. *ASME Journal of Applied Mechanics* **18,** 31–38.

Shindo, Y., Ohnishi, I. and Suzuki, S. (1993) Dynamic singular moments in a perfectly conducting plate with a through crack under a magnetic field. *ASME Mechanics of Electromagnetic Materials and Structures* (edited by J. S. Lee, G. A. Maugin and Y. Shindo) **AMD-161, MD-42,** 87–97.

Shindo, Y., Ohnishi, I. and Tohyama, S. (1995) The scattering of magnetic flexural waves of a conducting plate with a crack. *Applied Mechanics in the Americas* (edited by L. A. Godoy, S. R. Idelsohn, P. A. A. Laura and D. T. Mook) **I,** 471–476.

Sih, G. C. and Chen, E. P. (1977) Plates and shells with cracks. In *Mechanics of Fracture*, Vol. 3 (edited by G. C. Sih). Noordhoff International Publishing, Leyden, pp. 231–272.

APPENDIX A

Here, the effect of the magnetic field of $H_{0y} = H_0$, $H_{0x} = H_{0z} = 0$ on the flexural waves at normal incidence $\gamma = \pi/2$ is studied. The conducting plate is permeated by a static uniform magnetic field of $H_{0y} = H_0$. The incident flexural waves at normal incidence $\gamma = \pi/2$ are expressed as follows:

$$\begin{aligned}
\Psi_y^{i} &= \Psi_{y0} \exp[-i(ky+\omega t)],\\
\Psi_z^{i} &= \Psi_{z0} \exp[-i(ky)+\omega t)],\\
\varphi^{i} &= \varphi_0 \exp[-i(ky+\omega t)],\\
\psi^{i} &= \psi_0 \exp[-i(ky+\omega t)],\\
f^{i} &= f_0 \exp[-i(ky+\omega t)].
\end{aligned} \tag{A1}$$

The external fields outside the plate are

$$\begin{aligned}
h_x^{ei} &= 0,\\
h_y^{ei} &= iA_0 \exp(-kz) \exp[-i(ky+\omega t)] \quad (z \geqslant h)\\
&= -iA_0 \exp(kz) \exp[-i(ky+\omega t)] \quad (z \leqslant -h),\\
h_z^{ei} &= A_0 \exp(-kz) \exp[-i(ky+\omega t)] \quad (z \geqslant h)\\
&= A_0 \exp(kz) \exp[-i(ky+\omega t)] \quad (z \leqslant -h),
\end{aligned} \tag{A2}$$

where A_0 is an undetermined constant.

Making use of eqns (A2) and (29) renders the x, y-magnetic intensity components $h_x^{i}(x, y, \pm h, t)$, $h_y^{i}(x, y, \pm h, t)$ and the amplitude f_0

$$\begin{aligned}
h_x^{i}(x, y, \pm h, t) &= 0,\\
h_y^{i}(x, y, \pm h, t) &= \pm i f_0 \exp[-i(ky+\omega t)],\\
f_0 &= A_0 \exp(-kh).
\end{aligned} \tag{A3}$$

Substituting eqns (A1) and (A3) into eqns (33)–(35), we have

$$\begin{aligned}
\psi_0 &= 0,\\
\varphi &= -\frac{c_2 \kappa_0 H_0 \sigma_h (\omega/kc_2)^2}{(1+kh) - i\sigma_h(\omega/kc_2)} k\Psi_{z0},\\
k\varphi_0 &= \omega \kappa_0 f_0.
\end{aligned} \tag{A4}$$

Substituting eqns (A1) into eqns (45) and (46) yields

$$\frac{4}{3}\sigma_h(kh)^3\left(\frac{\omega}{kc_2}\right)^5+i\frac{4}{3}(kh)^3(1+kh)\left(\frac{\omega}{kc_2}\right)^4-\left[\left(\frac{8}{3}\frac{1}{1-\nu}+\frac{1}{9}\pi^2\right)\sigma_h(kh)^3+\frac{\pi^2}{3}\sigma_h(kh)+\frac{4}{3}(kh)^2(1+kh)\,\Gamma_h\right]\left(\frac{\omega}{kc_2}\right)^3$$
$$-i\left[\left(\frac{8}{3}\frac{1}{1-\nu}+\frac{1}{9}\pi^2\right)(kh)^3+\frac{\pi^2}{3}(kh)\right](1+kh)\left(\frac{\omega}{kc_2}\right)^2+\left[\frac{8}{3}\frac{1}{1-\nu}(kh)^2(1+kh)\Gamma_h\right.$$
$$\left.+\frac{2\pi^2}{9}\frac{1}{1-\nu}\sigma_h(kh)^3+\frac{\pi^2}{3}(1+kh)\Gamma_h\right]\left(\frac{\omega}{kc_2}\right)+i\frac{2\pi^2}{9}\frac{1}{1-\nu}(kh)^3(1+kh)=0, \quad \text{(A5)}$$

$$i\frac{\pi^2}{6}kh\Psi_{,y0}=-\left[\frac{\pi^2}{6}kh-2kh\left(\frac{\omega}{kc_2}\right)^2-2i\left(\frac{\omega}{kc_2}\right)\Gamma_h+\frac{\sigma_h(\omega/kc_2)^2\Gamma_h}{(1+kh)-i\sigma_h(\omega/kc_2)}\right]k\Psi_{,z0}. \quad \text{(A6)}$$

Figure A1 shows the variation of the phase velocity $\mathrm{Re}(\omega/kc_2)$ with the wave number kh for $\Gamma_h = 0.03$ ($B_0 = 12.2$ T), $\nu = 0.3$, $\sigma_h = 0.5$. The dashed curve refers to a quasistatic electromagnetic field. Figure A2 also shows the variation of the attenuation $-\mathrm{Im}(\omega/kc_2)$ with the wave number kh for $\Gamma_h = 0.03$ ($B_0 = 12.2$ T), $\nu = 0.3$, $\sigma_h = 0.5$. The effect of the magnetic field on $\mathrm{Re}(\omega/kc_2)$ is observed at wave number $kh < 0.3$. The result justifies the assumption of a quasistatic electromagnetic field.

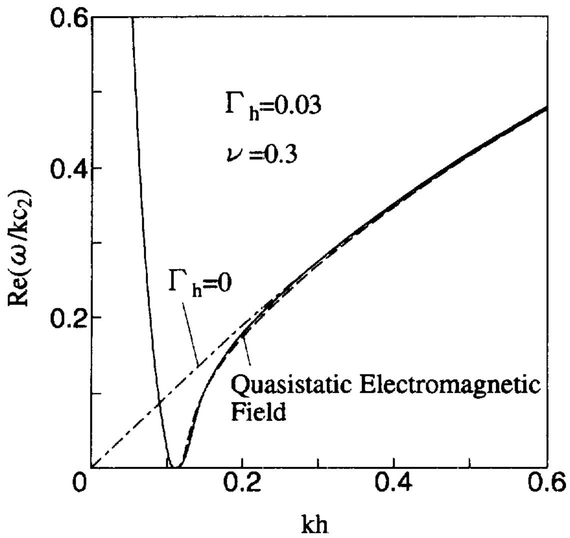

Fig. A1. Phase velocity $\mathrm{Re}(\omega/kc_2)$ vs wave number kh.

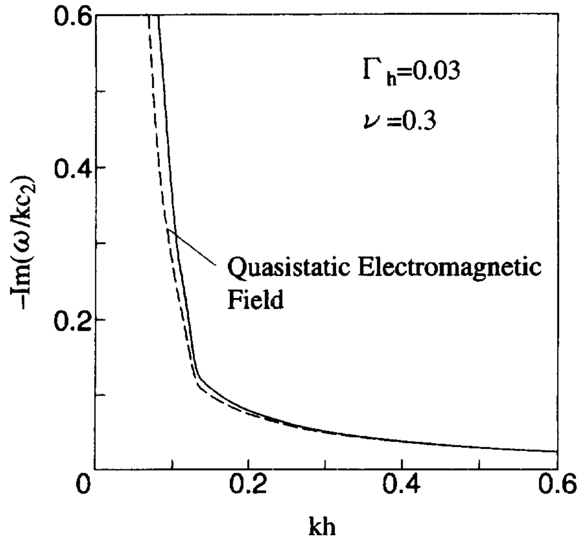

Fig. A2. Attenuation $-\mathrm{Im}(\omega/kc_2)$ vs wave number kh.

APPENDIX B

The dependency of the flexural wave on kh for three magnetic fields of $H_{0x} = H_0$, $H_{0y} = H_{0z} = 0$ (Case I), $H_{0y} = H_0$, $H_{0x} = H_{0z} = 0$ (Case II), $H_{0z} = H_0$, $H_{0x} = H_{0y} = 0$ (Case III) is studied. The conducting plate is permeated by a static uniform magnetic field $\mathbf{H}_0$. A quasistatic electromagnetic field is assumed for the plate.

(a) Case I ($H_{0x} = H_0$, $H_{0y} = H_{0z} = 0$)
Substituting eqns (A1) and (A3) into eqns (33), (34) and (51), we have

$$\psi_0 = i\omega\kappa_0 H_0 \Psi_{z0},$$
$$\varphi_0 = f_0 = 0. \tag{B1}$$

Substituting eqns (A1) into eqns (45) and (46) yields

$$\frac{4}{3}(kh)^2\left(\frac{\omega}{kc_2}\right)^4 + i\frac{4}{3}(kh)\Gamma_h\left(\frac{\omega}{kc_2}\right)^3 - \left[\left(\frac{8}{3}\frac{1}{1-\nu} + \frac{1}{9}\pi^2\right)(kh)^2 + \frac{\pi^2}{3}\right]\left(\frac{\omega}{kc_2}\right)^2$$
$$- i\frac{2\pi^2}{9}(kh)\Gamma_h\left(\frac{\omega}{kc_2}\right) + \frac{2\pi^2}{9}\frac{1}{1-\nu}(kh)^2 = 0, \tag{B2}$$

$$i\frac{\pi^2}{6}\Psi_{x0} = -\left[\frac{\pi^2}{6} - 2\left(\frac{\omega}{kc_2}\right)^2\right]k\Psi_{z0}. \tag{B3}$$

(b) Case II ($H_{0y} = H_0$, $H_{0x} = H_{0z} = 0$)
From eqn (60), we also have the frequency equation for Case II ($H_{0y} = H_0$, $H_{0x} = H_{0z} = 0$) as

$$\frac{4}{3}(kh)^3\left(\frac{\omega}{kc_2}\right)^4 + i\frac{4}{3}(kh)^2\Gamma_h\left(\frac{\omega}{kc_2}\right)^3 - \left[\left(\frac{8}{3}\frac{1}{1-\nu} + \frac{1}{9}\pi^2\right)(kh)^3 + \frac{\pi^2}{3}(kh)\right]\left(\frac{\omega}{kc_2}\right)^2$$
$$- i\left[\frac{8}{3}\frac{1}{1-\nu}(kh)^2 + \frac{\pi^2}{3}\right]\Gamma_h\left(\frac{\omega}{kc_2}\right) + \frac{2\pi^2}{9}\frac{1}{1-\nu}(kh)^3 = 0. \tag{B4}$$

(c) Case III ($H_{0z} = H_0$, $H_{0x} = H_{0y} = 0$)
Substituting eqns (A1) and (A3) into eqns (33), (34) and (51), we have

$$\varphi_0 = \psi_0 = f_0 = 0. \tag{B5}$$

Substituting eqns (A1) into eqns (45) and (46) yields

$$\frac{4}{3}(kh)^2\left(\frac{\omega}{kc_2}\right)^4 + i\frac{4}{3}(kh)\Gamma_h\left(\frac{\omega}{kc_2}\right)^3 - \left[\left(\frac{8}{3}\frac{1}{1-\nu} + \frac{1}{9}\pi^2\right)(kh)^2 + \frac{\pi^2}{3}\right]\left(\frac{\omega}{kc_2}\right)^2$$
$$- i\frac{\pi^2}{9}(kh)\Gamma_h\left(\frac{\omega}{kc_2}\right) + \frac{2\pi^2}{9}\frac{1}{1-\nu}(kh)^2 = 0, \tag{B6}$$

$$i\frac{\pi^2}{6}\Psi_{x0} = -\left[\frac{\pi^2}{6} - 2\left(\frac{\omega}{kc_2}\right)^2\right]k\Psi_{z0}. \tag{B7}$$

Figure B1 shows the variation of the phase velocity $\mathrm{Re}(\omega/kc_2)$ with the wave number kh for $\Gamma_h = 0.03$ ($B_0 = 12.2\,\mathrm{T}$), $\nu = 0.3$, $\sigma_h = 0.5$. The curves obtained for the x, z-direction magnetic fields (Cases I, III) almost coincide with the purely elastic case. Figure B2 also shows the variation of the attenuation $-\mathrm{Im}(\omega/kc_2)$ with the wave number kh for $\Gamma_h = 0.03$ ($B_0 = 12.2\,\mathrm{T}$), $\nu = 0.3$, $\sigma_h = 0.5$. The effect of the y-direction magnetic field (Case II) on flexural waves is more pronounced than those of x, z-direction magnetic fields (Cases I, III).

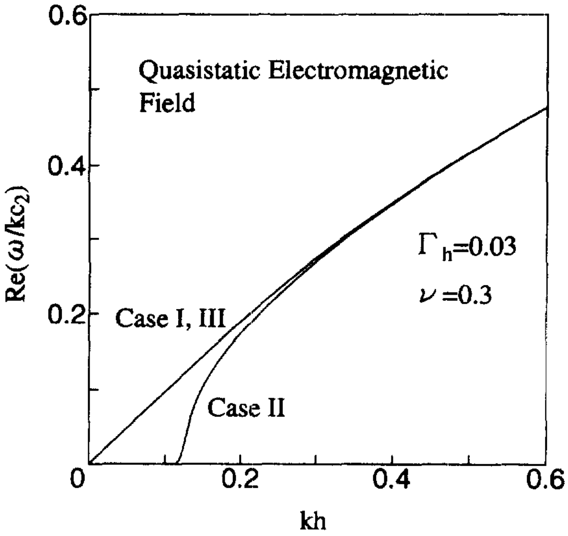

Fig. B1. Phase velocity $\mathrm{Re}(\omega/kc_2)$ vs wave number kh (quasistatic electromagnetic field).

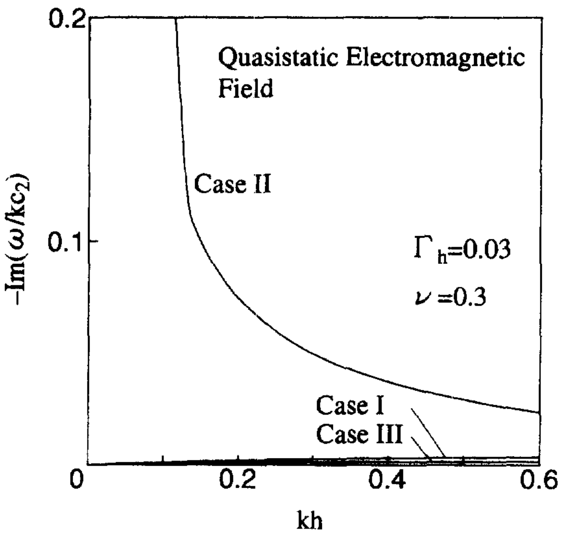

Fig. B2. Attenuation $-\mathrm{Im}(\omega/kc_2)$ vs wave number kh (quasistatic electromagnetic field).